http://dx.doi.org/10.21577/0103-5053.20170230

J. Braz. Chem. Soc., Vol. 29, No. 5, 1094-1104, 2018
Printed in Brazil - ©2018 Sociedade Brasileira de Química

Article

CO Tolerance and Stability of Proton Exchange Membrane Fuel Cells with Nafion® and Aquivion® Membranes and Mo-Based Anode Electrocatalysts

Renato C. Iezzi, Rapher D. M. Santos, Gabriel C. da Silva, Valdecir A. Paganin and Edson A. Ticianelli*

Instituto de Química de São Carlos, Universidade de São Paulo (USP), CP 780, 13560-970 São Carlos-SP, Brazil

This work presents a CO tolerance study of PtMo/C (70:30, Pt:Mo) and Pt/MoO_2-C anode catalysts on proton exchange membrane fuel cells (PEMFC) with Nafion® and Aquivion® ionomer membranes. Results denote improved activity for the hydrogen oxidation reaction (HOR) in the presence of CO on both anode catalysts at 85 °C. Experiments of identical location transmission electron microscopy evidenced very good stability of the Pt particles along an accelerate stress test (AST) applied to the Mo-based anode catalysts. However, a crossover of degradation Mo products originated in the anode and going to the cathode takes place along this anode AST, causing a PEMFC performance decay. A very little effect of the nature of the membrane, Nafion® or Aquivion®, is observed over these crossover phenomena. Results also denote that when operating at appropriate high temperatures (105 °C for Nafion® and 125 °C for Aquivion®), there is no need of incorporating unstable oxophilic transition metals on Pt to achieve improved CO tolerance on PEMFCs, when the CO level in the hydrogen fed is of the order of 100 ppm.

Keywords: CO tolerance, hydrogen oxidation, Nafion membrane, Aquivion membrane, Mo-based catalysts

Introduction

In nowadays the low availability of pure hydrogen to be used in the industry or as fuel for the hydrogen oxidation reaction (HOR) in fuel cells makes attractive the use of hydrogen generated by reforming fossil fuels, such as natural gas, methanol, ethanol, etc. However, the gas generated by this process contains CO as contaminant, which adsorbs on the surface of the platinum catalyst employed in the fuel cell anode, strongly affecting the hydrogen oxidation process, particularly in the proton exchange membrane fuel cell (PEMFC) system. For this reason, purification of hydrogen to remove CO has been an active area of research, and this initially comprises using the water-gas-shift process,[1] which allows a reduction of the CO content in the outlet hydrogen-reach gas stream to around 1.0% (v/v).[1] Unfortunately, this is not enough to make feasible utilization of the gas in low temperature fuel cells and thus more sophisticated purification procedures should be employed involving high temperature catalytic approaches such as partial oxidation,[2] palladium membrane filtering,[3] and hydrogen electrochemical compression/purification (HECP) redox procedures.[4] In the last case, impure hydrogen is fed to an acidic electrolyte membrane cell anode coupled to hydrogen evolution reaction (HER) cathode so that impure hydrogen is oxidized in the anode while pure hydrogen is produced in the cathode.[4] As in the case of the PEMFC, the HECP anode of such a system is poisoned by the supplied impure CO-containing hydrogen, reducing the efficiency of the system.

Therefore, the use of catalysts more resistant to CO contamination or finding other mechanisms that may contribute to a better performance of the anode in the PEMFC or in the HECP system is necessary.[5] In this way, oxophilic transition metals such as Ru or Mo are typically added to Pt to increase the CO tolerance of the electrocatalysts aiming at freeing Pt sites from the adsorbed CO.[6,7] Unfortunately, the insufficient durability reported for these catalysts still limit the large-scale commercialization of PEMFCs working with reformate fuel. This problem would be also reduced if a compression/purification system is coupled to the fuel cell or used to produce pure hydrogen, although the CO poisoning problem is transferred to this system. Advantages of using this late approach has been discussed previously.[4]

*e-mail: edsont@iqsc.usp.br
This paper is part of the PubliSBQ Special Issue "IUPAC-2017" (http://publi.sbq.org.br/).

Several previous works have been focused on developing CO tolerant catalysts.[8-12] For carbon supported bimetallic PtMo (60:40, Pt:Mo atomic proportion) materials, it has been found that a heat treatment at 600 °C under hydrogen atmosphere was very much beneficial to improve the stability and the activity for the hydrogen oxidation, either in the absence and in the presence of CO. Among a series of tungsten-based catalysts, tungsten carbide supported Pt catalyst showed reasonable performance and reliable stability in comparison to simple carbon supported PtW catalyst, although an uneven level of catalytic activity towards H_2 oxidation in the presence of CO is observed for the former as compared to Mo containing catalyst. Quaternary catalysts formed by applying first a suspension of PtMo/C catalyst to the electrode gas diffusion layer (GDL), followed by PtRu/C and finally by PtFe/C catalysts, have been also investigated. PtMoRu, PtMoFe, PtMoRuFe supported on carbon and Pt supported on Mo_2C/C exhibited similar CO tolerances, but better stability, as compared to the as-prepared PtMo supported on carbon. However, a dissolution of Mo, Ru, Fe and W species from the anodes and their migration toward the cathodes during the cell operation have been observed in all cases. This indicates that, although the fuel cell stability had been improved with the use of these anode materials, this improvement may not be enough when a long-term fuel cell operation perspective is considered.

It has been also found that increasing the PEM fuel cell temperature to values above 100 °C may provide great advantages regarding improvements of the oxygen reduction reaction (ORR) kinetics and the CO tolerance for the HOR.[10,12] In these works, results have shown that PEMFCs with either Pt/C, PtMo/C (60:40) and PW/C anodes present considerable improved CO tolerance by raising the cell operation temperature to 105 °C. However, some increase of the membrane resistivity had occurred because of the use of a Nafion® (DuPont) membrane for constructing the membrane and electrode assemblies (MEA). In this context, within the last decade, a new membrane, conceptually similar Nafion® had been developed (Aquivion®, Solvay), but containing shorter fluorocarbon chains, which result in high polymer crystallinity and hydrophilicity and thus high thermal stability and mechanical strength.[13,14] In fact, previous works have shown that when applied to PEMFC with pure H_2/O_2 reactants, the Aquivion® membrane had provided quite impressive performances for the PEMFC working at temperatures up to 130 °C,[15-18] this being a quite relevant fact when the CO tolerance issue is considered. The advantages of employing Aquivion® membranes have been also demonstrated on intermediate temperature PEM water electrolyzer systems.[19,20]

In this work, the CO tolerance process is investigated for anode electrocatalysts formed by as-prepared PtMo/C (70:30, Pt:Mo atomic proportion) and, for the first time, on Pt supported on a molybdenum oxide/carbon substrate (Pt/MoO_2-C). Effects on the CO tolerance considering the utilization of MEAs formed with Nafion® and Aquivion® membranes are characterized. Studies comprised catalyst physicochemical characterization by several techniques and single cell experimental investigation was carried out by obtaining steady state polarization curves and cyclic voltammograms. Changes in the fuel cell performance with temperature and the effect of catalyst particles properties after accelerate aging tests of the anodes are investigated by electrochemical impedance spectroscopy, Tafel diagrams, and identical location transmission electron microscopy (IL-TEM).

Experimental

Preparation of the electrocatalysts

The MoO_2-C support was prepared by first mixing ammonium heptamolybdate tetrahydrate $[(NH_4)_6Mo_7O_{24}{\cdot}4H_2O$, Merck] and Vulcan XC72-R carbon (Cabot), which was previously heat treated at 850 °C, 5 h, under argon atmosphere. The heat-treated carbon was first suspended in H_2O using an ultrasonic bath. The Mo precursor (C/Mo ratio = 3:1 m/m) was then added to this homogeneous suspension under continuous stirring. The mixture was dried in a water bath at approximately 90 °C, with stirring. After complete evaporation of the solvent, the material was placed into a furnace at 70 °C for a period of 12 h. The material was then thoroughly macerated and pretreated at 100 °C under an argon atmosphere for 1 h, followed by heat treatment at 550 °C also under argon for 5 h.[21] Incorporation of Pt nanoparticles to form the Pt/MoO_2-C electrocatalyst was made by reduction of a Pt precursor ($H_2PtCl_6.6H_2O$; Alfa Aesar) with formic acid.[22-24] In brief, a portion of as-prepared MoO_2-C support was weighed to give a final Pt/support ratio of 20 wt.% m/m and added to an aqueous solution of formic acid (0.5 M). This mixture was ultrasonically mixed to obtain a homogeneous suspension and then heated to 80 °C, with vigorous stirring. Then, the Pt precursor solution was added stepwise at intervals of 15 min. After complete reduction of the Pt precursor, the product was allowed to cool to room temperature, followed by filtration and washing with ultrapure water. The final product was then heated to 70 °C for 4 h to complete the drying. PtMo supported (20 wt.%) on Vulcan XC-72R (Cabot, previously heat-treated as described above) was prepared following a

previously described preparation procedure.[10-12] The method is essentially the same as that used for incorporation of Pt on MoO_2-C, except that the heptamolybdate tetrahydrate [$(NH_4)_6Mo_7O_{24}{\cdot}4H_2O$, Merck] was mixed to the Pt precursor to obtain a Pt:Mo atomic proportion of 70:30. Pt supported on Vulcan XC-72 carbon also with 20 wt.% metal/C was supplied by E-TEK.

Physical characterizations

The final metal contents of the MoO_2-C support as well as the final metal loadings (Pt and Mo) on the catalysts were evaluated by energy dispersive X-ray spectroscopy (EDX) in a scanning electron microscope LEO, 440 SEM-EDX system (Leica-Zeiss, DSM-960) with a microanalyzer (Link analytical QX 2000) and a Si (Li) detector using a 20 keV incident electron beam. Powder X-ray diffraction (XRD) patterns of the electrocatalysts were obtained to characterize the structural properties of the prepared materials using a RIGAKU XRD RU200B diffractometer using CuKα radiation in the 2θ range from 10 to 90°. The average crystallite sizes of Pt or PtMo in the catalyst samples were estimated by the Scherrer equation,[25] using the Pt (220) peak of the diffraction patterns. Homogeneity and particle size distributions of the prepared catalysts were investigated by transmission electron microscopy (TEM, JEOL JEM 2100 transmission electron microscope).

Electrochemical measurements

The electrochemical measurements were conducted in a single cell, using membrane electrode assemblies (MEAs) prepared with electrodes formed by carbon cloth-supported gas diffusion and catalyst layers. The materials and method for the preparation of MEA and its components are described in details elsewhere.[8-12,22-24] The gas diffusion layer comprised a mixture of carbon powder (Vulcan XC-72, Cabot) with 15 wt.% of polytetrafluoroethylene (PTFE, TE 3893, DuPont) placed on both sides of the carbon cloth substrate (Panex 30, Zoltek), each with a carbon + PTFE load of 3 mg cm^{-2}. The catalyst layer was deposited on one of the faces of the diffusion layers using a homogeneous suspension formed by appropriated amounts of Nafion® (Aldrich, 5 wt.%) or Aquivion® (D9825BS, Aldrich, diluted to 5 wt.% in water), the electrocatalysts (PtMo/C, Pt/MoO_2-C, and Pt/C) and isopropanol. The metal load in the electrode was 0.4 mg cm^{-2} for both, molybdenum-based anodes and Pt/C anodes/cathodes with the total geometric area of the electrodes equal to 5 cm^2. MEA was prepared by hot pressing the anode and cathode on both sides of the working membrane. In the case of Nafion® (Nafion 115, DuPont) the conditions were: temperature, 125 °C; pressure, 5 MPa, and pressing time, 2 min; for Aquivion (E87-12S, Solvay), the hot pressing was made at temperature of 160 °C, pressure 1 MPa, and pressing time of 2 min. The MEA was then placed between two high-density graphite plates with serpentine type gas distribution channels, with the electrode un-catalyzed diffusion layer placed in contact with these channels.

Fuel cell polarization measurements were carried out galvanostatically (Electronic Load HP 6050A) with the cell at 85 °C using the gases saturated with water at temperatures 15 °C for hydrogen (with or without 100 ppm CO) and 5 °C for oxygen above that of the cell. Details on the humidification system, temperature and pressure controls can be found elsewhere.[26] For all experiments, the cell was initially maintained at a potential of 0.7 V with pure H_2 and at 0.8 V with H_2/100 ppm CO, for 2 h each, prior to the data acquisition. At all times both, anode and cathode reactant streams, were kept at 1 bar partial pressure. This means that the total pressure in the chambers was 1 bar above the vapor pressure of water at the considered humidification temperature, that is: cell at 85 °C, H_2 humidifier at 100 °C and pressure 2.03 atm, O_2 humidifier at 90 °C and pressure 1.71 atm; cell at 105 °C, H_2 humidifier at 120 °C and pressure 3.01 atm, O_2 humidifier at 110 °C and pressure 2.45 atm; and cell at 125 °C, H_2 humidifier at 140 °C and pressure at 4.66 atm, O_2 humidifier at 130 °C and pressure 3.74 atm. The gas system was formed by a set of four mass flow controllers (MKS 1179A MFC and MKS 247D Four-Channel Readout unit), keeping the total flow rate at 250 mL min^{-1} for the cathode gas and 300 mL min^{-1} for the anode side. Pure oxygen was used as the cathode feed. All gases were purchased from White Martins.

Cyclic voltammetric experiments were conducted at room temperature for Pt/C, PtMo/C and Pt/MoO_2-C streams anodes, and Pt/C cathodes. These experiments were performed using a potentiostat-galvanostat (Solartron 1285) coupled to the standard fuel cell hardware, with the anode fed with argon functioning as the working electrode, while the cathode was constantly fed with hydrogen and used as both, counter electrode and the reversible hydrogen reference electrode (RHE).[9-12]

Accelerate aging test of these catalysts constituted of the anode potential cycling between 0.1 and 0.7 V, at a scan rate of the 50 mV s^{-1}. The cycling was performed at room temperature up to 5000 cycles. The performance of the MEA was evaluated before and after a group of potential cycles, by measuring polarization curves at different temperatures with the anode exposed at H_2 in absence and in presence of the 100 ppm of CO. Cyclic voltammetry was also made for the cathode by the same procedure as

for the anode, before and after the above-mentioned anode potential cycling.

Identical location transmission electron microscopy (IL-TEM)

The IL-TEM experiments were performed using a PEM single cell configuration. Initially, a catalyst ink was obtained by dispersion of 1 mg of the PtMo/C catalyst powder in 1 mL of isopropanol and 15 μL of Aquivion® ionomer solution (D98 25BS, diluted to 5 wt.%). A single drop of the catalyst ink was then deposited on a Lacey carbon gold grid (EMS, 300 mesh), and TEM images of selected regions were obtained. The TEM grid was then assembled as the working electrode of a PEM fuel cell. Briefly, a 1 cm^2 gas diffusion electrode containing 0.4 mg Pt cm^{-2}, and prepared in the same way as described above, was hot-pressed to an Aquivion® membrane at 160 °C and 1 MPa for 2 min. The TEM grid was then placed in contact with Aquivion® membrane, and the fuel cell assembly was clamped under 5 Nm. For the aging test, exactly the same procedure was applied as that used in the operational PEM single cell.

Results and Discussion

Physical characterization of the electrocatalysts

Results of elemental analyses obtained by EDX are given in Table 1. Results show that the real metal loading related to the metal/substrate ratios (for PtMo/C and Pt/MoO_2-C) are very close to the nominal value of 20 wt.%. Figure 1 shows the XRD patterns for the investigated catalyst and substrates. It is seen that the diffraction pattern for PtMo/C basically exhibit a peak of the carbon (2θ = 25°), and of the face centered cubic (fcc) crystalline structure of Pt at 2θ = 40°, 46°, 67°, 81°. For Pt/MoO_2-C, the diffraction patterns predominantly exhibit the peaks of the fcc crystalline structure of Pt, but some small peaks evidence the presence of the crystalline phase of MoO_2 at 26°, 37°, 53°,[21] (see also the JCPDS-32-671 standard). The average crystallite sizes of Pt in these catalysts were calculated from the Pt (220) diffraction peak, using the Scherrer equation and the values (2.4-3.8 nm) obtained were included in Table 1. The values evidence the formation of Pt nanoparticles with adequate sizes for fuel electrocatalyst applications.

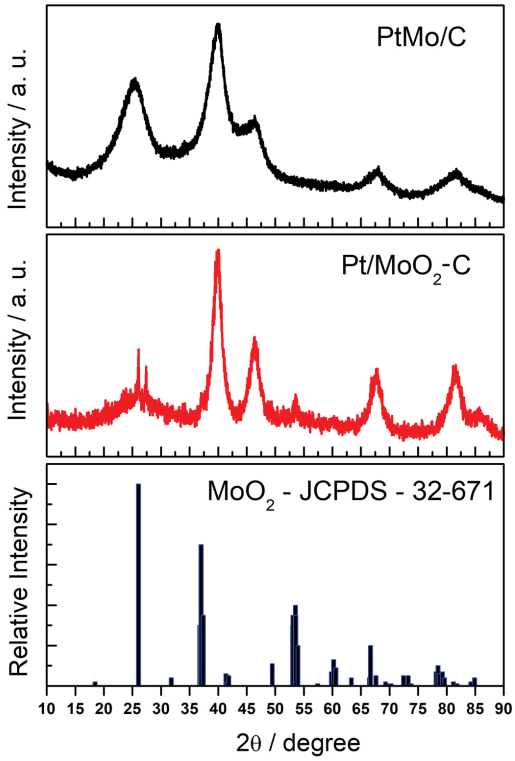

Figure 1. X-ray diffraction patterns of the electrocatalysts. Peaks from a JCPD-32-671 MoO_2 are included for comparison.

Figure 2 shows typical TEM images of the PtMo/C and Pt/MoO_2-C electrocatalysts, in which the corresponding Pt particle size histograms are included as inserts. Formation of remarkably uniform and disperse particles of Pt or eventually of PtMo alloy can be observed from the TEM images. The average metallic particle diameters calculated from these images are reported in Table 1, and these results evidence very good consistency with the average crystallites sizes estimated from XRD analyses. In Figure 2b it is seen that the contrast between the carbon black and molybdenum dioxide phases is not enough to clearly identify the MoO_2 particles, although the presence of such a phase was unequivocally evidenced by XRD. The metal particles supported on molybdenum oxide are

Table 1. Compositions and crystallite/particle sizes of various electrocatalysts

Electrocatalyst	EDX / wt.%			XRD	TEM
	Pt	Mo	C	Crystallite size / nm	Particle size / nm
PtMo/C	17.18	3.1	79.72	3.8	4.0
Pt/MoO_2-C	20.18	44.44	35.38	2.4	2.7

EDX: energy dispersive X-ray spectroscopy; XRD: X-ray diffraction; TEM: transmission electron microscopy.

somewhat more evenly distributed as compared to the PtMo particles supported on carbon black, suggesting that the dioxide surface facilitates into some extent the dispersion of the Pt particles.

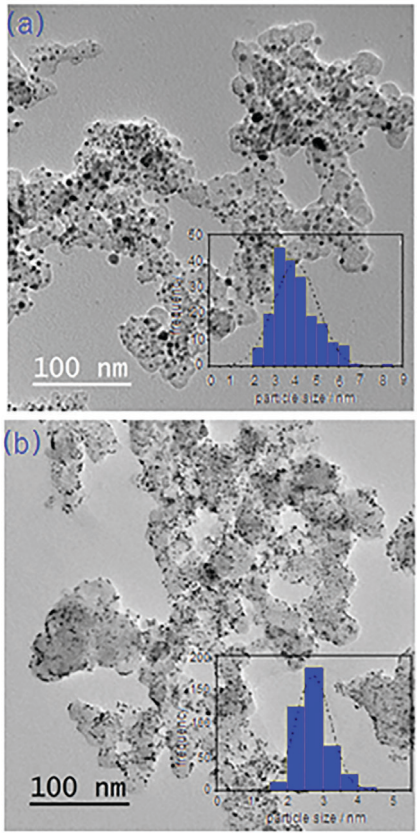

Figure 2. TEM images and particle size distributions of the (a) PtMo/C and (b) Pt/MoO_2-C electrocatalysts.

CO tolerance and catalyst stability at 85 °C

As mentioned before, the single cell anode cycling at 25 °C was used as an accelerated stress test (AST) for investigating the stability of the catalysts. The range of potential was 0.1 to 0.7 V *vs*. RHE and the scan rate was 50 mV s^{-1}; this procedure was repeated for up to 5000 potential cycles. Figure 3 shows polarization curves of PEMFCs with Nafion® membrane measured at 85 °C for the PtMo/C and Pt/MoO_2-C anodes supplied with pure H_2 and H_2/100 ppm CO, after various voltage cycles during the AST. The result for a Pt/C anode without cycling was included for comparison. Corresponding results for the cells with Aquivion® membrane are presented in Figure 4.

As can be seen in Figure 3, among the cells with Nafion® fed with pure H_2, that with the Pt/C anode showed the highest initial activity (highest cell potentials), followed by those with carbon supported PtMo/C materials and then by Pt/MoO_2-C. When the Aquivion® membrane is used, the results (Figure 4) with pure hydrogen before the anode cycling denote that the activities with PtMo/C and Pt/MoO_2-C anodes are improved in comparison to those of the Nafion® cells, resulting essentially the same as that of Pt/C.

The picture turns quite different when the anode feed is changed to the H_2/100 ppm CO mixture, as can be observed from the results in Figures 3 and 4. Now, the cells with Pt/C anode present the smallest current densities due to the Pt active sites blocking by the CO molecules, in agreement to what has been reported previously.[12] Compared to Pt/C, considerable improvement in the CO tolerance occurs when the Mo-containing catalysts are considered, for both Nafion® and Aquivion® PEMFCs. Results also denote that in the region of low current densities, all electrodes with both membranes essentially present the same response regarding the CO tolerance, but at high current densities a large fall of potential are observed for the cell with Aquivion® in all experimental conditions. This phenomenon is surely related to the appearance of diffusion limitation, possibly of oxygen in the cathode, where water is produced by the fuel cell reaction. The large affinity of Aquivion® to water explains why this water flooding occurs predominantly in Aquivion®-based MEAs.

When the accelerated stress tests are considered, results in Figures 3 and 4 evidence that in most situations the cell voltage decreases along the anode voltage cycling process at least up to ca. 3000 cycles, particularly when the anodes are supplied with H_2/100 ppm CO. After that the voltage stabilize, but in some cases a tendency of a slightly increase of voltage appears for cycles up to 5000. In summary, results in Figures 3 and 4 clearly denote that degradation processes take place in the anode catalysts, evidencing their inadequate stability for long-term practical applications. In spite of this, a slight improvement in the stability is observed for the cells with both membranes with the Pt/MoO_2-C anodes, as compared to those with PtMo/C.

Figure 5 shows cyclic voltammograms for the PtMo/C and PtMoO_2-C single cell anode electrocatalysts, obtained prior and in the course of the anode cycling. Results for the corresponding fuel cell cathodes are also included in this Figure. The well-known Pt-H adsorption/desorption peaks are apparent in all cases, especially in the cathodes, together with an oxidation peak appearing at ca. 0.45 V *vs*. RHE in the forward scan, and a reduction peak at ca. 0.42 V *vs*. RHE in the reverse scan. This redox couple is due to the change in the oxidation states of Mo from +4 to +6, and *vice versa*, during the oxidation/reduction processes, as reported in the literature.[12] Results denote that a decline in the intensity of these peaks takes place during the cycling process, suggesting occurrence of a partial dissolution of such species, particularly for up to 1000 cycles. After that, the

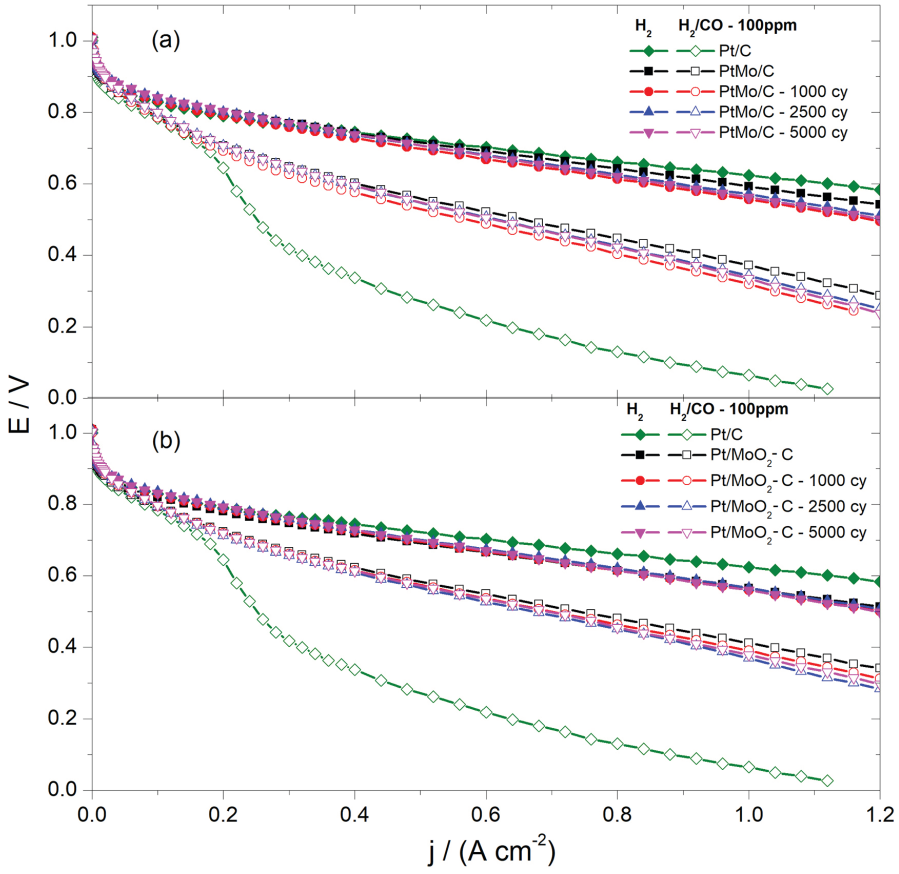

Figure 3. Polarization curves of PEMFC with Nafion® membrane measured at 85 °C for different catalysts after various voltage cycles during the AST: (a) PtMo/C and (b) Pt/MoO_2-C. Result for a Pt/C anode was included for comparison. Anodes were supplied with pure H_2 and H_2/CO mixture and the Pt/C cathodes were supplied with O_2.

current densities remain essentially constant, indicating that after the releasing of some Mo ionic species, further dissolution is very much reduced. These releasing of species are confirmed by the appearance of the Mo-related redox features in the single cell cathodes, which also evidence the crossover of the dissolved species from the anode to the cathode, after passing the membrane. The results also denote a very little effect of the nature of the membrane, Nafion® or Aquivion®, in the crossover tendencies.

Further insights on the effect of anode cycling were gained by the IL-TEM results, as shown in Figure 6 for the PtMo/C catalyst. From these results it is noted that, at least regarding the Pt particles, the material exhibit a very good stability throughout the 5000 AST cycles in the 0.1-0.7 V potential range. The red circles in Figure 6 indicate stable regions of the catalyst, where no significant changes in both, Pt nanoparticles and support material, are observed. This is the most predominant observation made from the IL-TEM analyses in several catalyst sample spots, although the results also point to the occurrence of minor agglomeration processes of the Pt particles, as highlighted by the green circles in Figures 6c and 6f. Nikkuni *et al.*[27] also evaluated the stability of Pt/C and Pt_3Co/C cathodic catalysts in a PEMFC environment using the IL-TEM technique. The authors used cathode cyclings between 0.1-0.9 V and 0.6-0.9 V (which includes the Pt-oxide features) as accelerated stress test, and, after cycling, noticed modifications on the Pt particles size, geometry and composition, in addition to the corrosion of the carbon support. The very large stability of the Pt nanoparticles, evidenced by IL-TEM in Figure 6, can be related to the mild aging test protocol employed here regarding Pt catalyst, since the upper potential limit used was restricted to 0.7 V, which is below the Pt-oxide features.

As in the case of the standard TEM results (Figure 2), no evidence of the presence of Mo-related phases could be seen from the IL-TEM features, and this is valid for the images obtained before and after the electrode cycling.

It is well known that the potential decay occurring during the PEMFC operation is determined by kinetics of the electrode reactions, particularly the ORR in the low current density region, ohmic drops strongly determined by the membrane resistivity appearing at intermediate current densities, and diffusion overpotentials appearing in the limit of high current densities. So far, the results presented here

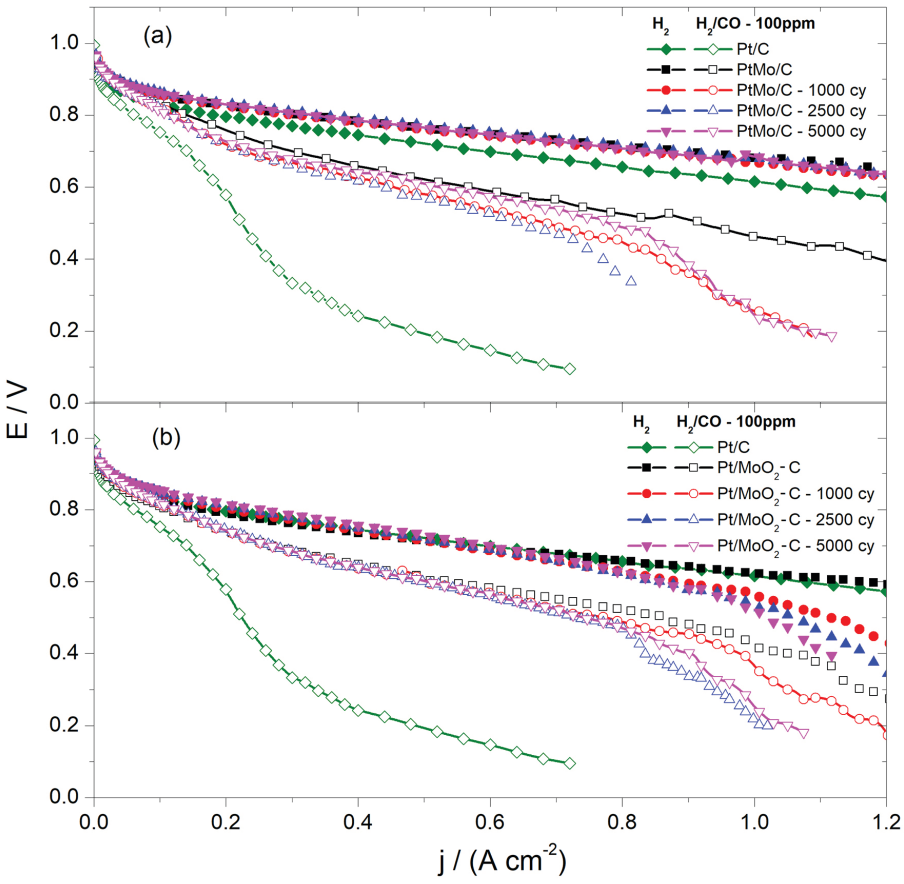

Figure 4. Polarization curves of PEMFC with Aquivion® membrane measured at 85 °C for different catalysts after various voltage cycles during the AST: (a) PtMo/C and (b) Pt/MoO_2-C. Result for a Pt/C anode was included for comparison. Anodes were supplied with pure H_2 and H_2/CO mixture and the Pt/C cathodes were supplied with O_2.

clearly evidence that the presence of Mo species in the anode is crucial for enhancing the CO tolerance and that there is a dissolution of such species from the anode and their migration though the membrane, reaching the cathode. Therefore, in principle, the decrease of the cell performance along the electrode cycling can be a consequence of all these phenomena, that is: the loss of Mo-species of the anode causing an increase of the anode overpotentials, an increase of the membrane resistance due to the presence of Mo-species causing an increase of ohmic drop effects, and/or a poisoning of Pt in cathode caused by the crossed Mo species, resulting in an increase of the ORR overpotentials.

The effects of Mo crossover to the membrane and to the cathode were characterized by means of electrochemical impedance measurements (reported in Figure 4) and by constructing Tafel plots from the polarization measurements at low current densities (reported in Figure 3). Diagrams are shown in Figures 7 and 8, respectively.

The Nyquist diagrams in Figure 7 exhibit the typical profiles observed for H_2/O_2 PEMFC,[10] either at open circuit or under operation (here at cell voltage of 0.8 V). At open circuit the diagrams are characteristic of a series resistive (R)-capacitive (C) circuit, with the intercept in the Z' axis (real impedance) occurring at high frequencies representing the total electric resistance of the cell, with the major contribution given by the membrane. At 0.8 V, the arc appearing at middle frequencies are for parallel R-C circuits with the radius mainly representing the charge transfer resistance of the oxygen electrode and the intercept in the high frequencies related to the membrane resistance, as in the previous case. In the present context, the more relevant information given by the results in Figure 7 is the invariance of the high frequency resistance, implying that the membrane resistance remain the same for the cell at open circuit, or under operation, and principally along the anode cycling, when some insertion of Mo-occurs. Therefore, a main conclusion reached from this experiment is that the decay of the fuel cell performance along the anode cycling cannot be related to any change of the membrane properties.

As mentioned above at low current densities, the fuel cell polarization is controlled by the ORR catalysis, particularly in the case of systems supplied with pure gases. In this way, Tafel diagrams shown in Figure 8 provide

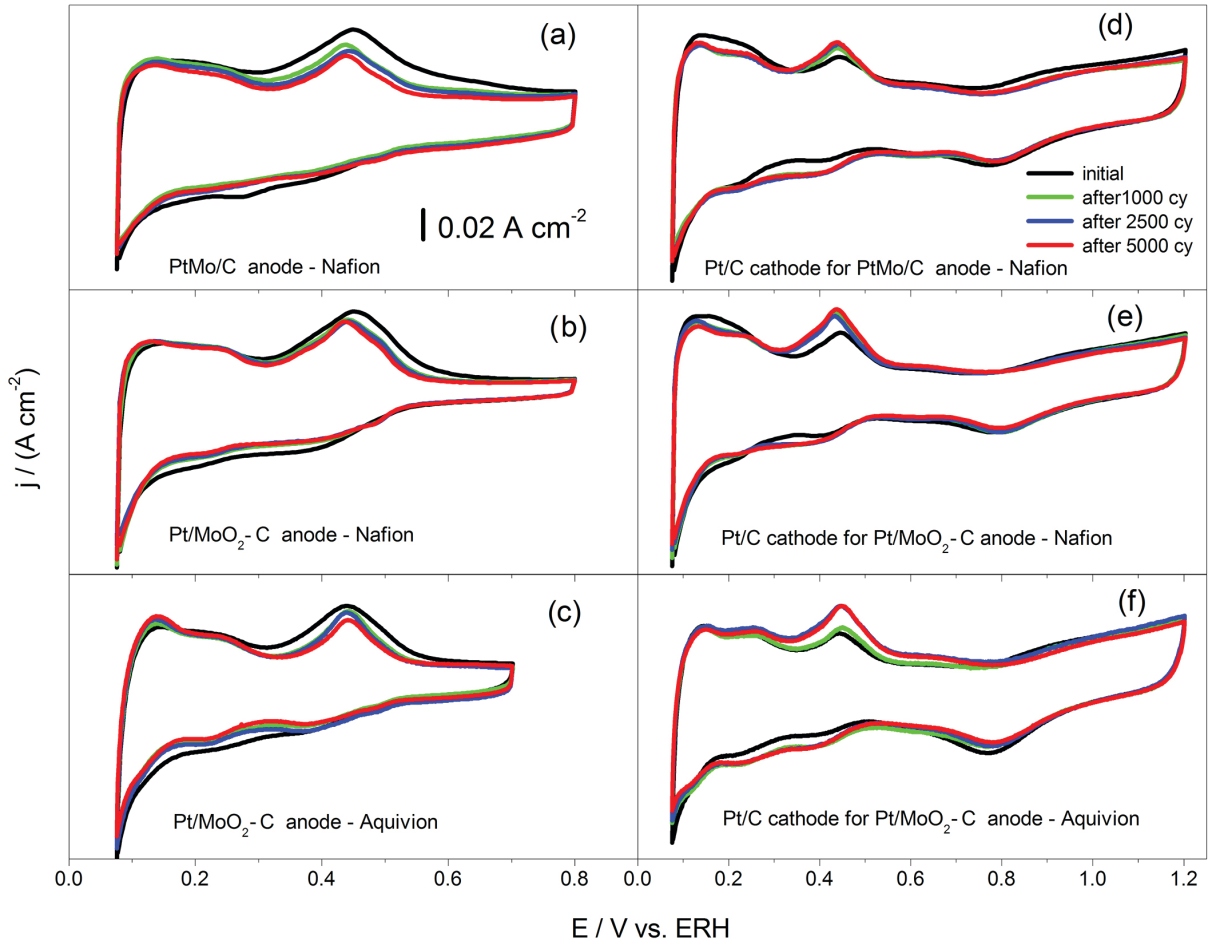

Figure 5. Cyclic voltammograms of anodes and cathodes obtained along the single cell anode cycling. Legend in the bottom of the Figure 5a denotes the sensitivity of the j axes in all figures.

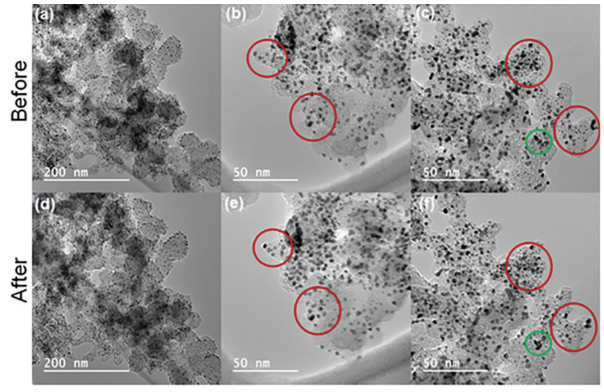

Figure 6. IL-TEM images before and after the anode AST 5000 cyclings.

information regarding the effect of contamination of Pt in the cathode with Mo species occurring along the anode cycling. These results clearly denote that an increase of the cell potentials takes place in the presence of these Mo species, evidencing an overall increase of the ORR kinetics. Such observation has been also made from rotating disk electrode experiments in sulfuric acid solutions.[21] In this way, the Tafel plots clearly demonstrate that the single cell

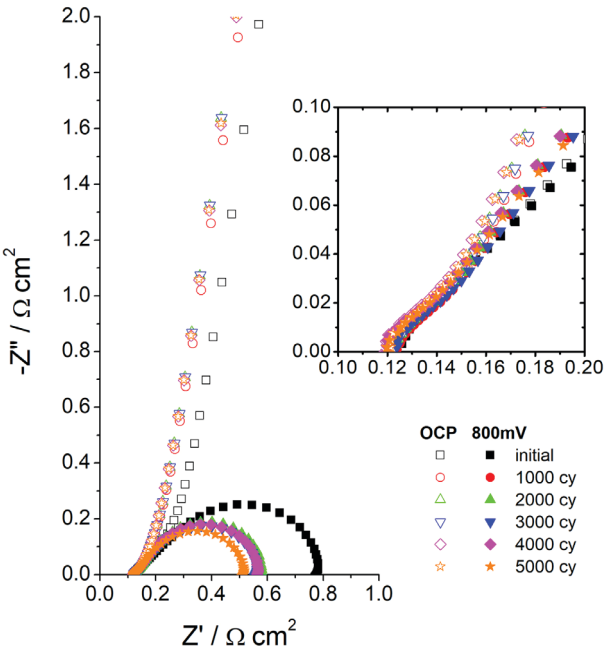

Figure 7. Nyquist plots of the single cell with Aquivion® membrane, PtMo/C in the anode and Pt/C in the cathode, obtained along the AST at 25 °C. Cell supplied with H_2 in the anode and O_2 in the cathode.

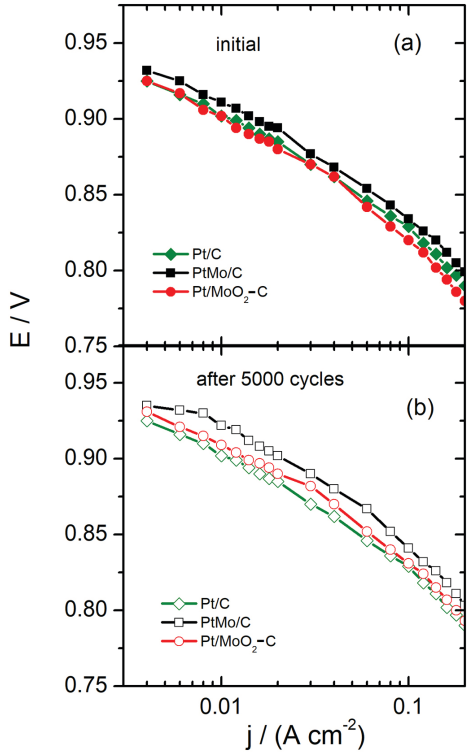

Figure 8. Tafel diagrams for the cells with Nafion® membrane and the Mo-based catalysts, (a) before and (b) after the electrode cycling (5000 cycles), for single cell electrodes supplied with pure H_2 and O_2.

performance decays due to the anode cyclings observed in Figures 3 and 4 are not related to the single cell oxygen electrode.

In summary, the present analysis regarding the properties of the anode catalyst and of the membrane and the cathode, before and after the anode AST, allows to conclude that the causes of the single cell performance decay occurring during the aging process are not related to the Pt content or morphology of the anode, the resistivity of the membrane or of the ORR electrocatalysis. The clear appearance of diffusion limitations at high current densities, particularly evident for the cell with Aquivion® MEAs (Figure 4), denotes that a reduction of the cathode/anode hydrophobicity and water flooding is the most important effect of Mo-species dissolution and crossover. In the case of Nafion® MEAs the effect is smaller, but also clearly evidenced, and this is consistent with the smaller water retention inside the electrode provided by the incorporated Nafion-ionomer.[13]

Effects of cell temperature for Nafion® and Aquivion® MEAs

Gases supplied to fuel cells with perfluorosulfonic acid membranes have to be constantly humidified to maintain their water saturation, so that the proton transfer processes within the sulfonated fluorocarbon chains present fast kinetics and the membrane maintains the required good conductivity. In that respect the cell temperature cannot be set to excessively high values to avoid large reductions in the membrane hydration and in the ionic conductivity. As mentioned before, to achieve higher proton conductivity at high temperatures, a good option has been the use of Aquivion® membrane.

Illustration of such phenomenon is made from the results of the polarization curves in Figure 9 obtained at 85, 105 and 125 °C for PEM single cells with the Aquivion® membrane, with Pt/C, PtMo/C, and $PtMoO_2$-C anodes fed with pure hydrogen and the Pt/C cathode with pure oxygen. Figure 9a shows the corresponding results of a Nafion® cell with the Pt/C anode and cathode. Contrarily to what is seen with the cell with Nafion® (see Figure 9a), the polarization results for the Aquivion®-based cells (Figures 9b and 9d) present similar performance, independently of the operation temperature, implying the existence of a balance regarding the effect of the temperature on the membrane properties and the reaction kinetics even at 125 °C. The consistency of such observation is confirmed by the similar trends seen

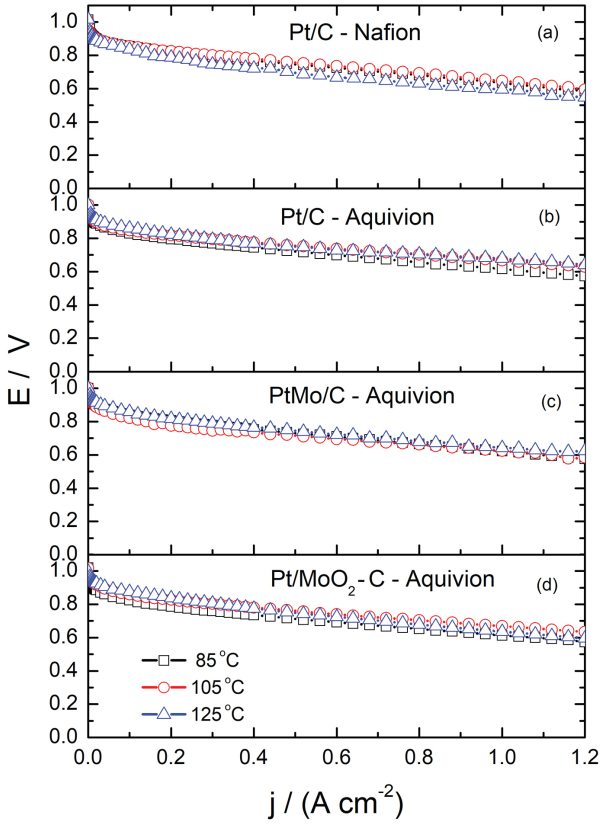

Figure 9. Polarization curves for PEMFCs operating at 85, 105 and 125 °C with: (a) Pt/C anode and cell with Nafion® membrane; (b) Pt/C, (c) PtMo/C and (d) Pt/MoO_2-C anodes and with Aquivion® E87-12S membrane. PEMFCs are supplied with pure hydrogen in the anode and pure oxygen in the Pt/C cathode.

when the PtMo/C and Pt/MoO_2-C catalyst are used in the Aquivion® fuel anode, as shown in Figures 9c and 9d.

CO tolerance results for PEMFCs at several temperatures and with Nafion® and Aquivion® MEAs with Pt/C anodes and Pt/C cathodes are shown in Figures 10a and 10b, respectively. As expected, in both cases the increase of temperature led to an increase of the anode CO tolerance, with the maximum cell performance obtained at 105 °C for the Nafion® and at 125 °C for the Aquivion® MEAs. This effect is related to the expected increase of the reactions kinetics, the increase of the membrane conductivity, and a decrease of adsorbed CO coverage on Pt with the increase of the cell temperature. However, the initial increase of the membrane conductivity is progressively reduced by the increasing water loss caused by the increase of temperature, until it reverts the tendency and compensates the positive effects of the other factors. This leads to maxima in the cell performance, which are reached at 105 °C for Nafion® and 125 °C for Aquivion®. In the same way as for the Pt anode, the best cell performance with Aquivion® MEA and Mo-based anodes is reached at 125 °C, but in the case of Pt/MoO_2-C the result at 125 °C is identical to that at 105 °C. This indicates that the CO tolerance of this anode catalyst is higher than that of PtMo/C because it can clean more effectively the Pt surface from adsorbed CO.

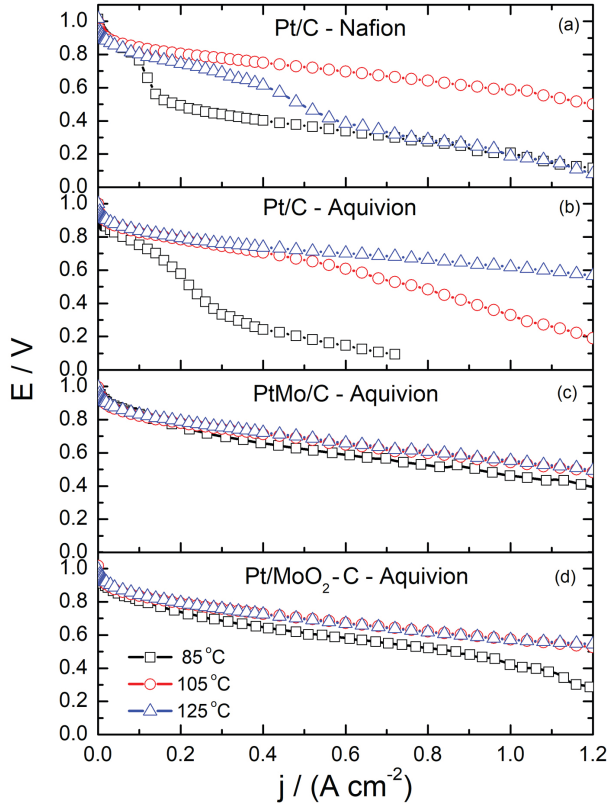

Figure 10. Polarization curves for PEMFCs operating at 85, 105 and 125 °C with: (a) Pt/C anode and cell with Nafion® membrane; (b) Pt/C, (c) PtMo/C, and (d) Pt/MoO_2-C anodes and cells with Aquivion® E87-12S membrane. PEMFCs are supplied with hydrogen 100 ppm CO in the anode and pure oxygen in the Pt/C cathode.

A final remark to be made is the fact that the Aquivion® fuel cell performances at 125 °C with Pt/C, PtMo/C and Pt/MoO_2-C anodes fed with H_2/100 ppm CO are essentially the same, with a little advantage of Pt/C. It should be also noted that these performance similarities must also include that of the Nafion® fuel cells working at 105 °C with Pt/C anode. This means that the CO tolerance of the anodes are essentially independent of the catalyst, implying that under these conditions there is no need of incorporating unstable oxophilic transition metals on Pt to achieve improved CO tolerance on PEMFCs, at least when the CO level in the hydrogen fed is of the order of 100 ppm. Further research is in course to check about the PEMFC performance stability for systems working under high temperatures with Nafion®, Aquivion®, H_3PO_4-impregnated polybenzimidazole membranes and CO concentrations higher than 100 ppm, ultimately reaching gas compositions similar to those of a practical reformer, which is also of high relevance for hydrogen compression/purification systems.

Conclusions

Single cell results evidence a considerable improvement of the CO tolerance when the Mo-containing catalysts are incorporated in fuel cell anodes, for both Nafion® and Aquivion® PEMFCs. However, degradation processes take place in these catalysts during AST aging, causing a deterioration of the PEMFC performance. Results denote that during the AST, there is dissolution of Mo species in the anode and their crossover to the cathode, after passing the membrane. A very little effect of the nature of the membrane, Nafion® or Aquivion®, is observed over these crossover phenomena. On the other hand, a slight improvement in the anode stability is seen for the cells with Pt/MoO_2-C anodes, as compared to those with PtMo/C. Considering the Pt nanoparticles and the carbon support, very good stability throughout the 5000 AST cycles is observed from the IL-TEM analyses in several catalyst spots, although results also point to the occurrence of minor agglomeration of the Pt particles.

Results also evidence that the dissolution of Mo-species causing a reduction of the HOR activity is the main factor causing the single cell performance decay along the anode ageing. It is also seen that no contributions to this decay related to changes in the Pt content in the anode, or to changes in the resistivity of the membrane or in the electrocatalysis of the ORR are minimal. Finally, it is observed that the Nafion® fuel cell performance with Pt/C anodes at 105 °C and those of Aquivion® fuel cells

at 125 °C with Pt/C, PtMo/C and Pt/MoO_2-C anodes fed either with H_2/100 ppm CO are essentially the same, with a little advantage of the cells with Pt/C anodes. This means that in these conditions the CO tolerance of the anodes is essentially independent of the catalyst, implying that there is no need of incorporating unstable oxophilic transition metals on Pt to achieve improved CO tolerance on PEMFCs, at least when the CO level in the hydrogen fed is of the order of 100 ppm.

Acknowledgments

The authors thank the CAPES (Coordenação de Aperfeiçoamento de Pessoal de Nível Superior, Brazil, Process No. 1653174) and FAPESP (Fundação de Amparo à Pesquisa do Estado de São Paulo, Brazil, Process No. 2013/16930-7) for financial supports.

References

1. Rangela, M. C.; Querino, P. S.; Borges, S. M. S.; Marchetti, S. G.; Assaf, J. M.; Vásquez, D. P. R.; Rodella, C. B.; Silva, T. F.; Silva, A. H. M.; Ramon, A. P.; *Catal. Today* **2017**, *296*, 262.
2. Rahimpoura, M. R.; Samimia, F.; Babapoor, A.; Tohidiana, T.; Mohebia, S.; *Chem. Eng. Process.* **2017**, *121*, 24.
3. Nyathi, T. M.; Fischer, N.; York, A. P. E.; Claeys, M.; *Faraday Discuss.* **2017**, *197*, 269.
4. Bouwman, P. J.; *ECS Trans.* **2016**, *75*, 503.
5. Baschuk, J. J.; Li, X.; *Int. J. Energy Res.* **2001**, *25*, 695.
6. Hajbolouri, F.; Andreaus, B.; Scherer, G. G.; Wokaun, A.; *Fuel Cells* **2004**, *4*, 160.
7. Yu, H.; Hou, Z.; Yi, B.; Lin, H. Z.; *J. Power Sources* **2002**, *105*, 52.
8. Hassan, A.; Carreras, A.; Trincavelli, J.; Ticianelli, E. A.; *J. Power Sources* **2014**, *247*, 712.
9. Hassan, A.; Paganin, V. A.; Carreras, A.; Ticianelli, E. A.; *Electrochim. Acta* **2014**, *142*, 307.
10. Hassan, A.; Paganin, V. A.; Ticianelli, E. A.; *J. Power Sources* **2016**, *325*, 375.
11. Hassan, A.; Paganin, V. A.; Ticianelli, E. A.; *Electrocatalysis* **2015**, *6*, 512.
12. Nepel, T. C. M.; Lopes, P. P.; Paganin, V. A.; Ticianelli, E. A.; *Electrochim. Acta* **2013**, *88*, 217.
13. Subianto, S.; Pica, M.; Casciola, M.; Cojocaru, P.; Merlo, L.; Hards, G.; Jones, D. J.; *J. Power Sources* **2013**, *233*, 216.
14. Gebert, M.; Merlo, L.; Arcella, V.; *ECS Trans.* **2011**, *30*, 91.
15. Aricò, A. S.; Stassi, A.; Gatto, I.; Monforte, G.; Passalacqua, E.; Antonucci, V.; *J. Phys. Chem. C* **2010**, *114*, 15823.
16. Aricò, A. S.; Di Blasi, A.; Brunaccini, G.; Sergi, F.; Dispenza, G.; Andaloro, L.; Ferraro, M.; Antonucci, V.; Asher, P.; Buche, S.; Fongalland, D.; Hards, G. A.; Sharman, J. D. B.; Bayer, A.; Heinz, G.; Zandonà, N.; Zuber, R.; Gebert, M.; Corasaniti, M.; Ghielmi, A.; Jones, D. J.; *Fuel Cells* **2010**, *10*, 1013.
17. Xiao, P.; Li, J.; Tang, H.; Wang, Z.; Pan, M.; *J. Membr. Sci.* **2013**, *442*, 65.
18. Marrony, M.; Beretta, D.; Ginocchio, S.; Nedellec, Y.; Subianto, S.; Jones, D. J.; *Fuel Cells* **2013**, *13*, 1146.
19. Skulimowska, A.; Dupont, M.; Zaton, M.; Sunde, S.; Merlo, L.; Jones, D. J.; Rozière, J.; *Int. J. Hydrogen Energy* **2014**, *39*, 6307.
20. Siracusano, S.; Baglio, V.; Moukheiber, E.; Merlo, L.; Aricò, A. S.; *Int. J. Hydrogen Energy* **2015**, *40*, 14430.
21. Martins, P. F. B. D.; Ticianelli, E. A.; *ChemElectroChem* **2015**, *2*, 1298.
22. Pereira, L. G. S.; Paganin, V. A.; Ticianelli, E. A.; *Electrochim. Acta* **2009**, *54*, 1992.
23. Santiago, E. I.; Paganin, V. A.; Carmo, M.; Gonzalez, E. R.; Ticianelli, E. A.; *J. Electroanal. Chem.* **2005**, *575*, 53.
24. Camara, G. A.; Giz, M. J.; Paganin, V. A.; Ticianelli, E. A.; *J. Electroanal. Chem.* **2002**, *537*, 21.
25. Radmilovic, V.; Gasteiger, H. A.; Ross, P. N.; *J. Catal.* **1995**, *154*, 98.
26. Paganin, V. A.; Freire, T. J. P.; Ticianelli, E. A.; Gonzalez, E. R.; *Rev. Sci. Instrum.* **1997**, *68*, 3540.
27. Nikkuni, F. R.; Dubau, L.; Ticianelli, E. A.; Chatenet, M.; *Appl. Catal. B* **2015**, *176-177*, 486.

Submitted: October 20, 2017
Published online: December 13, 2017